Atmos. Meas. Tech., 5, 723–734, 2012
www.atmos-meas-tech.net/5/723/2012/
doi:10.5194/amt-5-723-2012

Atmospheric Measurement Techniques

Global distributions of C_2H_6, C_2H_2, HCN, and PAN retrieved from MIPAS reduced spectral resolution measurements

A. Wiegele, N. Glatthor, M. Höpfner, U. Grabowski, S. Kellmann, A. Linden, G. Stiller, and T. von Clarmann

Karlsruher Institut für Technologie, Institut für Meteorologie und Klimaforschung, Karlsruhe, Germany

Correspondence to: A. Wiegele (andreas.wiegele@kit.edu)

Received: 29 July 2011 – Published in Atmos. Meas. Tech. Discuss.: 19 August 2011
Revised: 7 February 2012 – Accepted: 3 April 2012 – Published: 13 April 2012

Abstract. Vertical profiles of mixing ratios of C_2H_6, C_2H_2, HCN, and PAN were retrieved from MIPAS reduced spectral resolution nominal mode limb emission measurements. The retrieval strategy follows that of the analysis of MIPAS high resolution measurements, with occasional adjustments to cope with the reduced spectral resolution under which MIPAS is operated since 2005. MIPAS measurements from January 2005 to January 2010 have been analyzed with special emphasis on October 2007. Largest mixing ratios are found in the troposphere, and reach 1.2 ppbv for C_2H_6, 1 ppbv for HCN, 600 pptv for PAN, and 450 pptv for C_2H_2. The estimated precisions in case of significantly enhanced mixing ratios (including measurement noise and propagation of uncertain parameters randomly varying in the time domain) and altitude resolution are typically 10 %, 3–4.5 km for C_2H_6, 15 %, 4–6 km for HCN, 6 %, 2.5–3.5 km for PAN, and 7 %, 2.5–4 km for C_2H_2.

1 Introduction

The Michelson Interferometer for Passive Atmospheric Sounding (MIPAS) (Fischer et al., 2008) instrument onboard the European Space Agency's (ESA) Envisat research satellite (http://envisat.esa.int/earth/www/area/index.cfm?fareaid=6) measures atmospheric limb emission in the mid-infrared (IR) spectral region in five spectral bands between 685 cm^{-1} and 2410 cm^{-1}. From the spectra retrieval of more than thirty atmospheric constituents is possible. From June 2002 to March 2004 MIPAS measured at a spectral resolution of 0.025 cm^{-1} (high spectral resolution, HR). After a failure of the interferometer slide operation resumed in January 2005 at a degraded spectral resolution of 0.0625 cm^{-1} (reduced spectral resolution, RR), however, at improved horizontal and vertical sampling. Retrievals of temperature and stratospheric constituents, namely H_2O, O_3, HNO_3, CH_4, N_2O, $ClONO_2$ and ClO from reduced spectral resolution spectra already have been published by von Clarmann et al. (2009b).

In this paper we present RR retrievals of gases which are important in the upper troposphere in the context of atmospheric pollution by industrial sources and biomass burning: C_2H_6, C_2H_2, HCN, and PAN. These species are particularly useful to trace intercontinental transport of pollution plumes (e.g. Liang et al., 2007; Wolfe et al., 2007), to assess chemical plume aging (e.g. Talbot et al., 1996; Xiao et al., 2007), to assign polluted air masses to particular pollution events (e.g. von Clarmann et al., 2007; Glatthor et al., 2007, 2009; Shim et al., 2007), and to assess their potential transport into the stratosphere (e.g. Randel et al., 2010). While these species have already successfully been retrieved from MIPAS high resolution spectra, this paper presents the retrieval strategy adapted to MIPAS reduced resolution spectra along with extensive characterization in terms of error estimates and spatial resolution. Results and diagnostics are discussed in comparison with those obtained from the MIPAS high resolution spectra. These retrievals are performed with the IMK-IAA research processor (von Clarmann et al., 2003).

2 Measurements

The MIPAS instrument measures atmospheric emission in mid-IR in limb geometry from a sun-synchronous polar orbit of 98.5° inclination and 10:00 a.m. downward leg equator crossing local time (LT) at an altitude of about 800 km. All of the measurements described in this paper are performed in

the so-called reduced resolution nominal mode with 27 tangent altitudes per limb scan. The scanning pattern varies with latitude; the lowermost nominal tangent altitude is 5 km close to the poles and 12 km at the equator. The uppermost tangent altitudes vary between 70 and 77 km, respectively. The tangent altitude increment increases with altitude from 1.5 km at the lowermost part of the scan pattern to 4 km at the uppermost altitudes (cf. http://www.atm.ox.ac.uk/group/mipas/rrmodes.html). Measurements containing a cloud signal are identified with a scheme as proposed by Spang et al. (2004). The along-track sampling is about 400 km. During one day roughly 1400 profiles are measured in about 14.4 orbits. For our retrievals, the measured spectra are apodised with the Norton and Beer (1976) "strong" apodization function.

3 Retrieval

The retrieval follows the strategy described in von Clarmann et al. (2003), i.e. radiative transfer calculations are performed with the Karlsruhe Optimized and Precise Radiative Transfer Algorithm (KOPRA, Stiller et al., 2002). dedicated spectral regions (so-called "microwindows") are used instead of the entire spectral band in order to gain computational efficiency and to reduce the signal of interfering species (von Clarmann and Echle, 1998; Echle et al., 2000). An empirical continuum emission as well as a zero-level calibration correction is jointly fitted to the spectra to reduce the sensitivity of the retrieval to weakly wavenumber-dependent inaccuracies of radiative transfer modelling and calibration. A regularization scheme based on a Tikhonov-type first order finite differences scheme is used to stabilise the retrieval (Steck and von Clarmann, 2001; Tikhonov, 1963). The used spectroscopic dataset is HITRAN04 (High Resolution Transmission) (Rothman et al., 2005) and corresponding updates (e.g. Allen et al., 2005).

Since the species under assessment do not possess prominent spectral signatures, interference with lines of other species is a major issue. In order to minimise the propagation of uncertainties in the abundances of interfering species, either vertical profiles resulting from a preceding retrieval of the interferents in a different spectral region are used to model their contribution to the spectral signal (so-called "pre-fit"), or the abundances of the interferents are jointly fitted with the abundances of the target species (so-called "joint-fit") (cf. Table 1). Temperature, tangent altitude information and mixing ratios of the major contributors to the infrared spectrum were taken from von Clarmann et al. (2009b). The retrieval grid has a 1 km spacing up to 44 km and is coarser above (2 km up to 70 km and 5 km up to 120 km). For radiative transfer modelling, a horizontally homogeneous atmosphere in case of trace gas mixing ratios is assumed. However, for temperature, a linear horizontal variation was allowed in a range of 400 km around the nominal geolocation of the limb scan. This improves the accuracy of the retrieval (Kiefer et al., 2010), and in many cases helps to reduce the number of convergence failures.

Table 1. Prefitted (P) and jointly fitted (J) parameters. Spectral shift, temperature, line-of-sight and HNO_3 are prefits at all retrievals.

species	C_2H_6	HCN	PAN	C_2H_2
H_2O	P	P	J	P
O_3	P	J	J	J
CH_4	P			P
N_2O		P		P
$ClONO_2$	P	P	J	P
ClO	P	P	P	
N_2O_5		P		P
HNO_4	P	P		
CFC-11	P		P	
CFC-12	P			
NO_2		P		
C_2H_6		P	P	
PAN				P
HCN			P	
CFC-22			J	
C_2H_2			J	
CH_3CCl_3			J	
CCl_4			J	

3.1 Retrieval of C_2H_6

C_2H_6 has been measured from space by the Atmospheric Trace Molecule Spectroscopy Experiment (ATMOS) (Rinsland et al., 1987), the Atmospheric Chemistry Experiment-Fourier Transform Spectrometer (ACE-FTS) (Rinsland et al., 2005), and MIPAS. The retrieval procedure for the MIPAS HR spectra of C_2H_6 was developed by von Clarmann et al. (2007) and Glatthor et al. (2009). The retrievals of C_2H_6 from reduced resolution spectra are performed as described there. Despite the different spectral resolution and tangent altitude grid, their retrieval setup proved robust also for the reduced resolution measurements and required no major modification. The highest tangent altitude used is 52 km, the lowest one depends on cloud top altitude. The microwindows used are located between 811.5 cm^{-1} and 835.75 cm^{-1} (see Table 2).

The regularization chosen leads to the averaging kernels as shown in Fig. 1. While the peak values of the averaging kernels are decreasing with altitude and the averaging kernels are broadened, they are still well-behaved in a sense that they are roughly symmetric and peak at the nominal altitudes. The only undesirable feature is the strong negative oscillation of the 5 km averaging kernel at 10 km, resulting from optically thick conditions.

The altitude resolution, calculated as half width of the rows of the averaging kernel matrix, is about 3 km at lowermost altitudes and degrades to about 9 km at 20 km and above

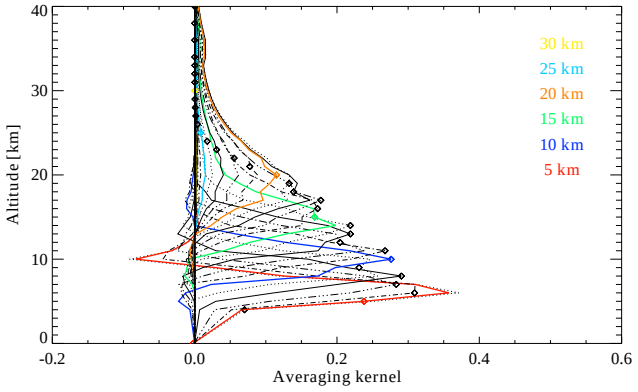

Fig. 1. Rows of the averaging kernel matrix for C_2H_6, evaluated for a limb scan recorded at 80° S, 162° E on 10 October 2009. Selected nominal altitudes are highlighted by colours.

Table 2. Microwindows and upper altitude limits (in brackets) for MIPAS reduced resolution nominal mode retrievals (cm^{-1}).

$C_2H_6^*$ (52 km)	HCN* (68 km)	$C_2H_2^*$ (35 km)
811.5000–811.8750	715.5000–718.0000	730.7500–731.3125
814.1875–814.5000	732.4375–735.8125	738.4375–738.7500
816.8750–817.1250	737.5000–741.6250	743.1250–743.5625
819.3750–819.8125	744.3125–747.8125	750.1875–750.4375
822.1875–822.5000	750.1875–753.8750	755.1250–759.8750
824.5000–825.1250	756.0000–760.7500	762.0000–767.0625
827.3750–827.7500	767.8125–770.9375	767.1250–772.1250
829.9375–830.4375	773.6250–776.8125	773.5625–778.5000
831.4375–831.7500	779.3750–782.7500	782.8750–787.8125
832.6250–833.1250		789.8750–790.1250
833.9375–834.2500		799.1250–799.4375
835.5000–835.7500		1309.3750–1311.7500
		1316.1875–1316.3750
PAN (33 km)		
775.000–787.0000		
794.500–800.0000		

* Not all spectral gridpoints are used at each altitude, depending on interference by other species.

(see Table 4). Since the altitude resolution of HR measurements remains better than 7 km at higher altitude and reaches similar values in the troposphere, the altitude resolution of RR is a little weaker than that of HR. The horizontal information smearing of the measurement was estimated using the method by von Clarmann et al. (2009a). The horizontal information smearing calculated as the halfwidth of the horizontal component of the 2-D averaging kernel is approximately 410 km at altitudes below 15 km and about 480 km above (see Table 4). The horizontal information is displaced with respect to the nominal geolocation of the limb measurement by 78 km at 7 km altitude towards the satellite, and 70 km at 12 km, respectively.

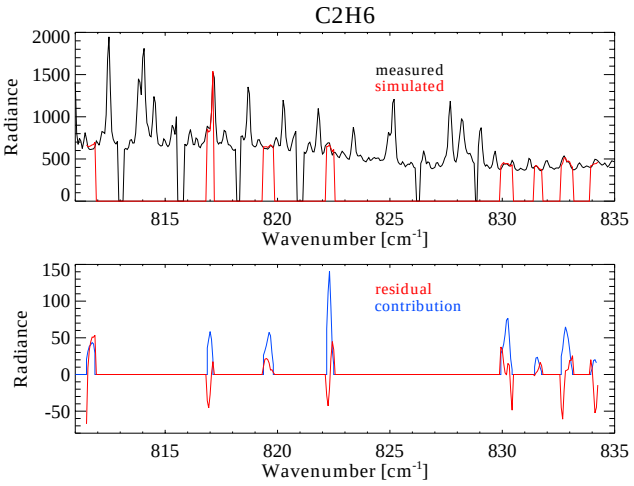

Fig. 2. Measured (black) and simulated (red) spectrum of a single C_2H_6 measurement (upper panel) at 11.0 km. The difference between both is the residual (red) and is plotted in the lower panel. The spectral contribution of C_2H_6 (blue) is calculated as difference between a forward simulation of the atmosphere taking into account all contributing gases and the corresponding forward simulation excluding C_2H_6. Radiances are given in $nW/(cm^2\,sr\,cm^{-1})$. Zero radiances in calculated spectra and residual spectra reflect data points excluded from the analysis. The root mean squares (RMS) difference for the shown set of microwindows is 29.5 $nW/(cm^2\,sr\,cm^{-1})$.

In Fig. 2 the measured and modelled spectrum and the fit residual of both are displayed. In comparison to the residual the spectral contribution of C_2H_6 is shown in the lower part of the plot. The noise eqivalent spectral radiance (NESR) in the spectral range is about 10.4 $nW/(cm^2\,sr\,cm^{-1})$ (referring to the apodised spectra) while the root of mean squares (RMS) of the residual is 29.5 $nW/(cm^2\,sr\,cm^{-1})$. The part of the residuals not explained by the noise is attributed to parameter uncertainties discussed below and to the effect of the regularization scheme used, but nevertheless the spectral contribution of C_2H_6 exceeds the residual.

The estimated retrieval errors are dominated by measurement noise at the lowermost altitudes (cf. Table 3) and by propagation of ozone uncertainties at altitudes at and above 15 km. The total random (noise plus propagation of random parameter uncertainties) retrieval error is estimated at 76 to 158 pptv for altitudes of 8 to 12 km. This corresponds to a relative error of about 11 % at altitudes up to 12 km for measurements of quite large mixing ratios, such as in a pollution plume. The accuracy of the C_2H_6 is also affected by the uncertainty of spectroscopic data. This, however, is hard to estimate, since the various available data sets differ by up to a factor of two (cf. von Clarmann et al., 2007 and references therein), while related uncertainty estimates are much more optimistic. We use the data set of the HITRAN 2004 edition (Rothman et al., 2005) that reports an uncertainty of 5–10 % for most major lines and ≥20 % for some minor lines. These

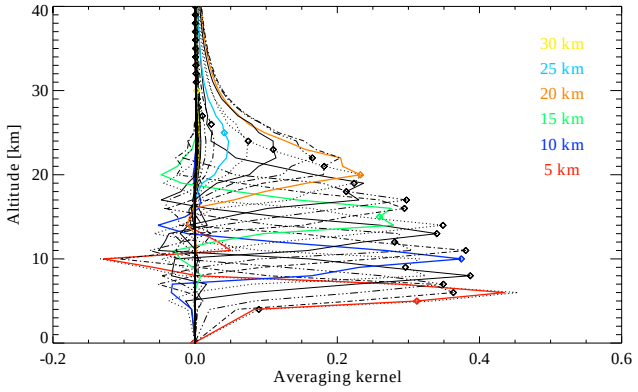

Fig. 3. As Fig. 1 but for C_2H_2.

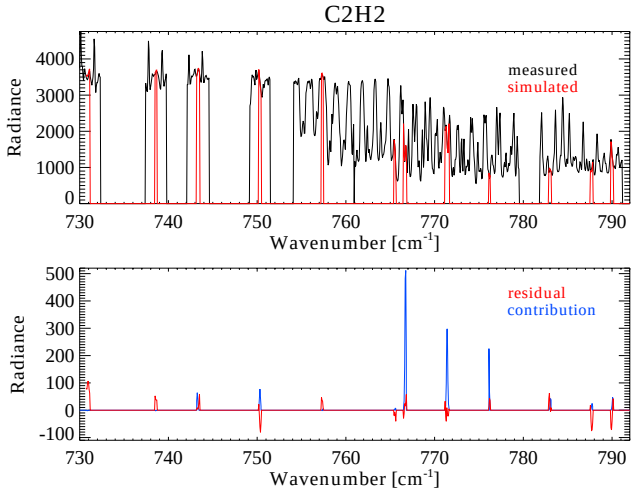

Fig. 4. As Fig. 2 but for C_2H_2. The RMS difference for the shown set of microwindows is 46.22 nW/(cm^2 sr cm^{-1}).

spectroscopic uncertainties, however, have no impact on the relative patterns.

3.2 Retrieval of C_2H_2

Space-borne measurements of C_2H_2 have been reported by Rinsland et al. (1987) (ATMOS) and Rinsland et al. (2005) (ACE-FTS). A method retrieving C_2H_2 from MIPAS HR spectra was developed by Glatthor et al. (2007). Their C_2H_2 is fitted jointly with PAN between 775 cm^{-1} and 800 cm^{-1}. In contrast, we use C_2H_2 emissions in the 730.75 cm^{-1} and 787.8125 cm^{-1} spectral region (see Table 2), and we use pre-fitted PAN mixing ratios. In our retrieval, ozone is the only jointly fitted species (see Table 1).

The averaging kernels are displayed in Fig. 3. The vertical resolution of RR is better than 4 km below 18 km and worse than 8 km above 24 km. Negative oscillations are even more pronounced than those of C_2H_6. The vertical resolution is slightly improved compared to HR at altitudes below 18 km but worse above. The horizontal information smearing

Table 3. Total errors of the retrievals in pptv and percent and the five largest contributing error sources (pptv); LOS = line of sight elevation pointing error; ILS = instrumental line shape uncertainty; gain = radiometric gain calibration error. The errors are calculated for a single biomass burning plume location with enhanced mixing ratios of all gases.

C_2H_6	8 km	10 km	12 km	15 km	20 km
total	160	140	82	170	140
total (%)	11.2	10.6	8.9	82.6	$\gg$100
noise	150	130	71	70	61
LOS	51	48	33	0.8	0.2
PAN	35	32	13	6	1.2
gain	6.9	6.1	0.2	13	24
O_3	5.7	4.8	18	150	130

C_2H_2	8 km	10 km	12 km	15 km	20 km
total	30	27	20	9.5	9.5
total (%)	7.1	6.8	6.8	54.1	>100
noise	23	20	8.5	8.9	6.6
LOS	18	18	18	1.8	2.1
PAN	4.8	4.2	4.2	0.7	0.1
ILS	4.4	4.0	2.3	0.7	1.6
gain	3.9	3.7	1.4	0.8	1.3

HCN	8 km	12 km	16 km	20 km	30 km	40 km
total	120	96	35	32	54	76
total (%)	13.0	11.9	14.4	17.9	21.7	68.2
noise	43	36	23	25	32	42
LOS	100	83	14	5.5	3.6	7.9
gain	23	16	0.8	7.0	7.8	3.2
T	21	16	0.6	1	5.4	4.9
ILS	13	12	11	7.3	10	7.5

PAN	8 km	10 km	12 km	15 km	20 km
total	45	31	27	19	18
total(%)	6.9	5.2	5.7	>100	$\gg$100
noise	36	30	16	17	15
LOS	24	5.6	21	7.4	5.1
gain	6.3	1.8	2.7	1.6	4.5
ILS	5.4	2.8	1.9	0.8	0.2
HNO_3	1.7	1.4	0.8	3.5	4.3

is 229 km (for both see Table 4). The calculated horizontal information displacement at 7 km altitude is 73 km towards the satellite, and at 12 km 71 km, respectively.

The spectral contribution of C_2H_2 is much higher than that of C_2H_6 (see Fig. 4). While an NESR of 22.2 nW/(cm^2 sr cm^{-1}) is expected and the residual RMS is 46.22 nW/(cm^2 sr cm^{-1}), the contribution of C_2H_2 to the simulated spectrum exceeds the residual by a factor of up to ten, depending on the transition.

The retrieval error of the C_2H_2 retrieval is dominated by noise and tangent altitude uncertainties (see Table 3). The total random retrieval error is estimated at 20 to 30 pptv for altitudes of 8 to 12 km. The total random retrieval error at

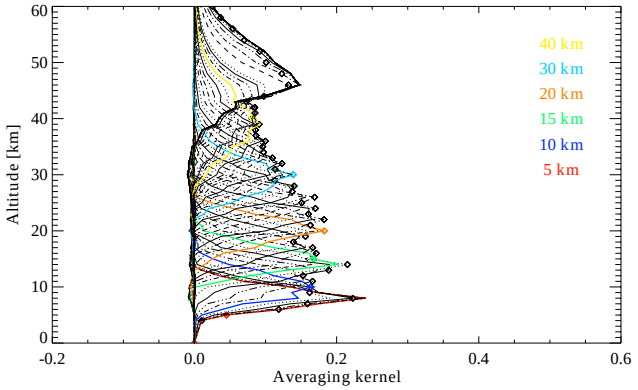

Fig. 5. As Fig. 1 but for HCN.

mixing ratios typical for plume conditions (about 350 pptv) is at about 7 %. Again, relative errors are increasing strongly above the altitudes of significant prominence, here at about 13 km. As a further source of systematic error, a spectroscopic data uncertainty of 2–5 % has to be considered (Rothman et al., 2005).

3.3 Retrieval of HCN

HCN measurements from space are available from the ATMOS (Rinsland et al., 1998), ACE-FTS (Rinsland et al., 2005), the Mesospheric Limb Sounder on Aura (MLS-Aura) (Pumphrey et al., 2006) and MIPAS. First MIPAS full resolution retrievals of HCN were developed by Glatthor et al. (2007). In contrast to their retrieval setup, here we jointly fit O_3 instead of using pre-fitted O_3 mixing ratios. This leads to a better agreement between measured and modelled radiances and hints at inconsistencies of ozone spectroscopic data in the spectral region used for the HCN retrieval and that used for the regular O_3 retrievals. Since ozone uncertainties are the dominating parameter error source of the HCN retrieval, this additional effort is justified. Further, we use a different set of microwindows, to cope with worse spectral interference problems at the reduced spectral resolution (cf. Table 2). The use of the original microwindow set of the full resolution retrievals would lead to a high bias of HCN at altitudes above 30 km.

The averaging kernels of HCN yield smaller peak values than those of C_2H_6 and thus are wider (Fig. 5), but there is no issue with negative oscillations. The altitude resolution is about 4 km at lowermost altitudes and degrades to 6 km at 25 km. Above 40 km, it is worse than 10 km (see Table 4). Compared to HCN HR measurements (Glatthor et al., 2007), the altitude resolution at RR is slightly improved. The horizontal information smearing is approximately 425 km at altitudes below 15 km and about 500 km above (see Table 4). The horizontal information displacement is 93 km at 7 km altitude towards the satellite, and 92 km at 12 km, respectively.

Table 4. Vertical resolution (upper part) and horizontal information smearing (lower part), calculated as full width at half maximum of the corresponding averaging kernels calculated according to von Clarmann et al. (2009a).

altitude	7 km	12 km	20 km	34 km
vertical resolution				
C_2H_6	3.0 km	4.0 km	8.0 km	9.0 km
C_2H_2	2.5 km	3.5 km	6.0 km	9.0 km
HCN	4.0 km	4.0 km	6.0 km	8.0 km
PAN	2.5 km	3.0 km	6.0 km	7.5 km
horizontal information smearing				
C_2H_6	416 km	403 km	480 km	485 km
C_2H_2	388 km	382 km	524 km	549 km
HCN	438 km	417 km	487 km	497 km
PAN	307 km	327 km	473 km	513 km

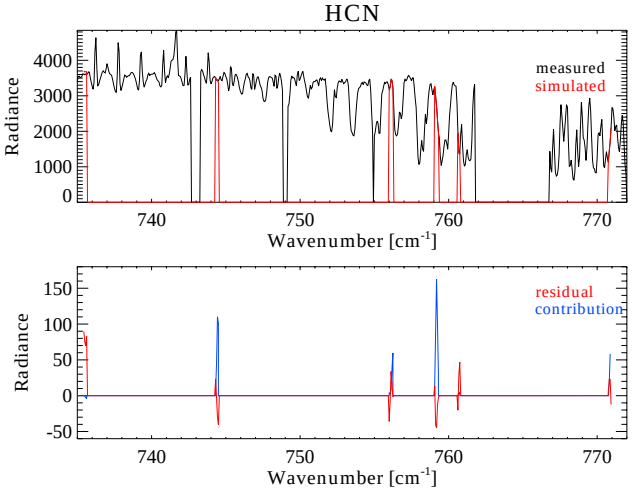

Fig. 6. As Fig. 2 but for HCN. The RMS difference for the shown set of microwindows is 40.0 nW/(cm^2 sr cm^{-1}).

The residual between the measured and the modelled spectrum is plotted in Fig. 6 along with the measured and the modelled spectrum. While NESR is at about 13.4 nW/(cm^2 sr cm^{-1}) the RMS of the residual is at about 40.0 nW/(cm^2 sr cm^{-1}). The spectral contribution of HCN outmatches the residual by up to a factor of three, depending on the particular transition.

Random parameter errors are the main error source at most altitudes (see Table 3). Depending on altitude, the error budget is dominated by tangent altitude pointing uncertainties, measurement noise, spectral shift, and at a few altitudes interference by N_2O_5. The total random retrieval error is estimated at 95 to 115 pptv for altitudes of 8 to 12 km and at 32 to 54 pptv for altitudes of 15 to 30 km. The relative error is less than 15 % at lowermost altitudes and less than 25 % up

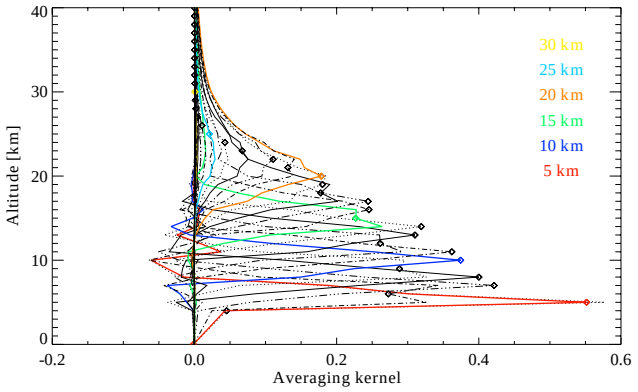

Fig. 7. As Fig. 1 but for PAN.

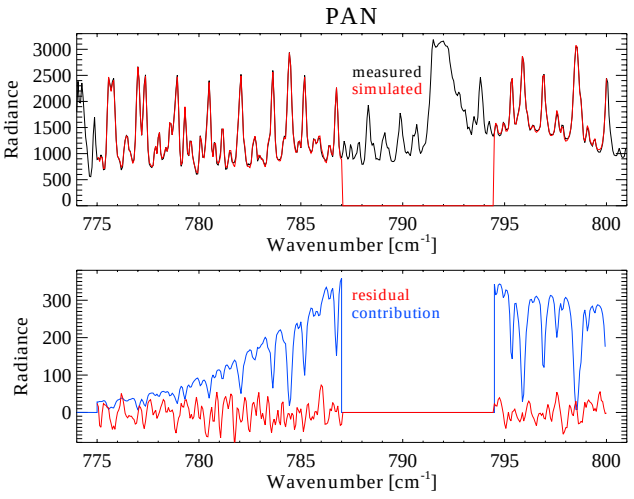

Fig. 8. As Fig. 2 but for PAN. The RMS difference for the shown set of microwindows is 26.9 nW/(cm^2 sr cm^{-1}).

to 30 km. The spectroscopic data error, including both line strengths and linewidth uncertainties, is estimated at 5–10 %.

3.4 Retrieval of PAN

Space-borne measurements of peroxyacetyl nitrate (PAN) are available from ACE-FTS (Coheur et al., 2007), from MIPAS high spectral resolution measurements (Glatthor et al., 2007), the Infrared Atmospheric Sounding Interferometer (IASI) (Coheur et al., 2009). Another set of MIPAS PAN retrievals from high resolution spectra has been published by Moore and Remedios (2010).

The PAN retrieval from reduced resolution MIPAS spectra has been modified with respect to the PAN retrievals developed for full resolution MIPAS spectra by Glatthor et al. (2007). Like for HCN retrievals, O_3 is now jointly retrieved instead of being prefitted. The microwindows have been adjusted slightly to the reduced resolution spectra (cf. Table 2). Small microwindows in the 775 cm^{-1}–800.0 cm^{-1} spectral region were merged. This led to a better determined retrieval of the background continuum, since in our retrieval the jointly fitted background continuum assigns one continuum variable per microwindow. However, the gap between 790.5 cm^{-1} and 794.5 cm^{-1} has been kept in order to avoid interference problems with the CO_2 Q-branch at 792 cm^{-1}.

The altitude resolution of the retrievals which is about 2.5 km at lowermost altitudes, degrades to 4 km at 15 km, and to more than 7 km at 25 km and above (cf. Fig. 7 and Table 4). The altitude resolution of HR PAN retrievals is comparable but does not go below 4 km. The horizontal information smearing is approximately 315 km at altitudes below 15 km and about 495 km above (see Table 4). The horizontal information is displaced by 65 km at 7 km altitude towards the satellite, and 60 km at 12 km, respectively.

Figure 8 exhibits the spectra, the spectral residual and the contribution of PAN at a single retrieval. The expected NESR is about 10.8 nW/(cm^2 sr cm^{-1}) and the RMS of the residual is about 26.9 nW/(cm^2 sr cm^{-1}). The contribution of PAN exceeds the RMS clearly.

Dominating error sources are measurement noise and tangent altitude pointing uncertainty (Table 3). The total random retrieval error is estimated at 27 to 45 pptv for altitudes of 8 to 12 km. The total relative error in lowermost altitudes is about 7 % and less. The band intensity uncertainty is estimated at 3.2 % and the spectroscopic data error is reported to be 5–10 % for most major lines.

4 Results

Within this study, all four species discussed above were analyzed for the period from April 2006 to October 2007. In the following, we show selected examples of measurements in October 2007. This period has been selected because of the plumes which are formed by biomass burning regularly at October in southern midlatitudes (Singh et al., 1996; Glatthor et al., 2009). Single orbit volume mixing ratios (vmr) as well as monthly mean vmrs based on 10 selected days corresponding to 10 541 measuremed limb sequences of spectra will be shown. The monthly means have been calculated for latitude-longitude bins of 5 times 15°.

4.1 C_2H_6

Ethane (C_2H_6) is the most important non-methane hydrocarbon (Singh et al., 2001) in the troposphere. Its sources are supposed to be anthropogenic emission or production by biomass burning. While most recent papers (e.g. Xiao et al., 2008) estimate industrial activity as dominating, former ones (Rudolph, 1995) propose equality between both sources. Dominating sinks are reaction with OH in the troposphere and with atomic chlorine (Cl) in the stratosphere (Aikin et al., 1982).

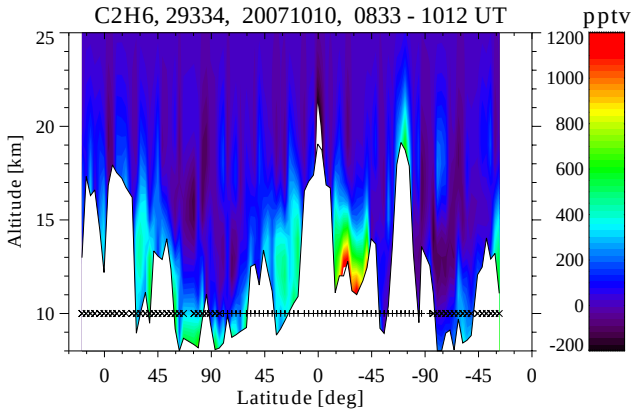

Fig. 9. Single orbit measurements of C_2H_6 vmr. Mixing ratios are plotted versus altitude and latitude. "x"-symbols represent nighttime, while "+"-symbols are daytime measurements.

Mixing ratios of C_2H_6 measured by MIPAS close to the tropopause often reach values of 400 pptv, and up to 1.2 ppbv at highly polluted air masses at single measurements. In Fig. 9 such an air mass can be found at about 30° S when the satellite passes this latitude for the first time at the shown orbit. For HR measurements (Glatthor et al., 2009) mixing ratios up to 700 pptv at single locations were found.

Monthly means are calculated for latitude-longitude bins of 5 times 15°. We observed the maximium monthly mean mixing ratios of C_2H_6 in October 2007 at about 800 pptv. For monthly means of the same month in different years the RR mixing ratios fit well to the HR mixing ratios. In the extratropics, less prominent but nevertheless significant enhancements of C_2H_6 can be found at northern latitudes especially above Asia (Fig. 10) (note that the distributions are shown here for lower altitudes than for the tropics). These generally higher values in the northern hemisphere may be attributed to anthropogenic activities. The amplitudes of mixing ratios between plume regions and adjacent locations in other months usually are in the order of 400 pptv (Table 5). The estimated precision of single measurements is smaller by about a factor of four. This implies that the precision even of single profile retrievals is by far sufficient to detect natural variability.

Five years of zonal means of MIPAS reduced spectral resolution C_2H_6 measurements are shown in Fig. 11. An annual cycle is clearly visible at most latitudes. In some regions, its amplitude is about 200 pptv, which extends the estimated single profile precision by a factor of two.

In October 2003 Glatthor et al. (2009) found mixing ratios of about 600 pptv in the upper troposphere close to Africa, while our RR measurements in October 2007 show mixing ratios of about 800 pptv above the southern Atlantic Ocean in air masses advected from the African continent at similar latitudes (Fig. 10). Enhancements in these regions in 2003 have been attributed to intercontinental transport of pollutants, particularly from biomass burning in the Amazonas

Table 5. Amplitude of local variability at 12 km altitude versus single profile precision as a measure of detectability. All values are given in pptv.

Gas	Amplitude	Biomass Burning Plume	surrounding Mixing Ratios	single Measurement Precision
C_2H_6	400	800	400	82
C_2H_2	150	200	50	20
HCN	400	600	200	96
PAN	350	350	50	27

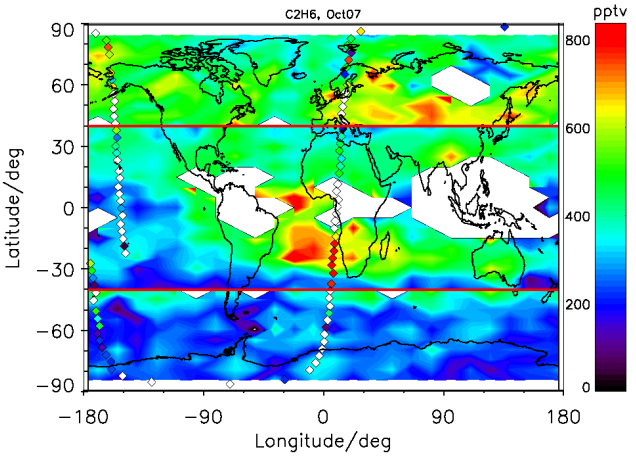

Fig. 10. Global monthly means of C_2H_6 vmr for October 2007. Between the red lines (40° N and S) C_2H_6 vmr is shown at 12 km, at latitudes poleward of 40° at 8 km. This display is chosen to represent the upper troposphere at all latitudes. The monthly means are calculated for latitude-longitude bins of 5 times 15°. The symbols mark the location of the C_2H_6 single orbit plot figured above. The colours of the symbols represent the mixing ratios along the single orbit measurements at 12 or 8 km depending on latitude. White symbols or areas indicate either mixing ratios below zero or cloud contamination.

region (von Clarmann et al., 2007). These authors found mean mixing ratios of C_2H_6 of approx. 600 pptv in a biomass burning plume measured by MIPAS HR between late October and mid of November 2003. Facing the large interannual variability in the five years of MIPAS RR data, the small differences with respect to the MIPAS HR data set do not hint at any biases between MIPAS HR and RR retrievals. The ACE-FTS (Atmospheric Chemistry Experiment-Fourier Transform Spectrometer) instrument on SCISAT detected mixing ratios up to 1.2 ppbv in July 2004 (Rinsland et al., 2007) and up to 1.5 ppbv at single measurements in autumn 2004 (Rinsland et al., 2005). These values are well consistent with the 1.2 ppbv MIPAS measurement in a highly polluted air mass. Means of three months of ACE C_2H_6 measurements (JJA 2005) result in maximum zonal mixing ratios of about 700 pptv in northern midlatitudes and 8 km (González

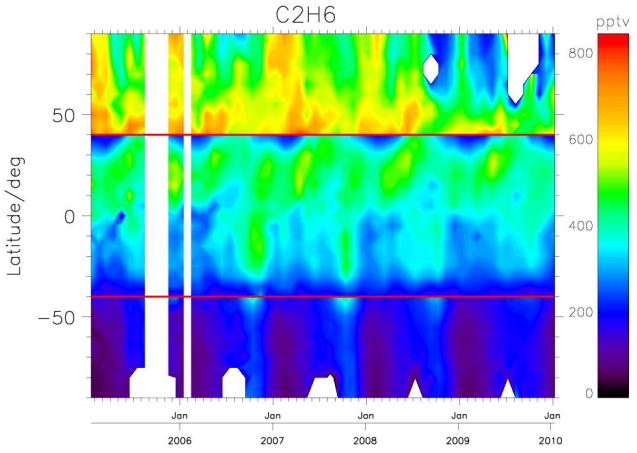

Fig. 11. Time series of C_2H_6 vmr. Zonal monthly mean (5° width) mixing ratios are plotted versus latitude and time. For the red lines see Fig. 10.

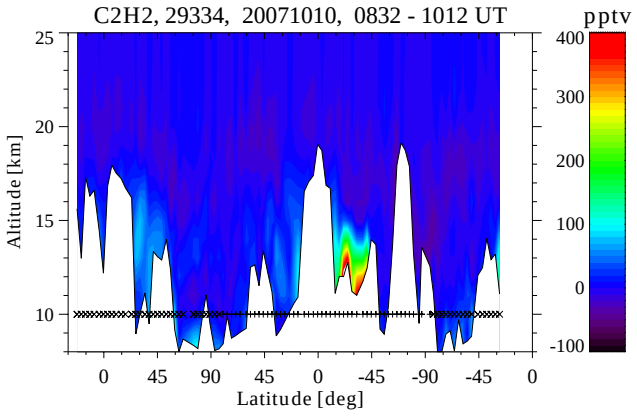

Fig. 12. As Fig. 9 but for C_2H_2.

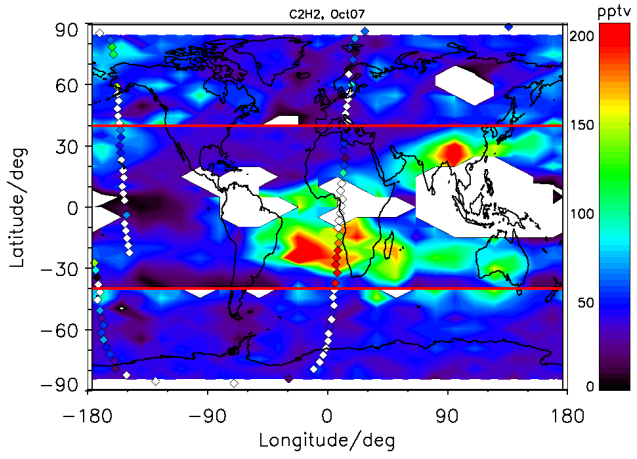

Fig. 13. As Fig. 10 but for C_2H_2.

Abad et al., 2011). This again agrees well with our MIPAS measurements (see monthly zonal means in Fig. 11).

4.2 C_2H_2

The sources and sinks of ethine (C_2H_2) are similar to those of ethane, although the relative importance of biomass burning is larger (Singh et al., 1996).

Similar to the pollutant discussed before, MIPAS measurements of C_2H_2 show significantly increased mixing ratios at 30° S at the orbit plotted in Fig. 12. Mixing ratios up to 400 pptv are reached there, while few other measurements reach about 100 pptv and most of them are close to zero. Glatthor et al. (2007) found mixing ratios of C_2H_2 at single MIPAS HR measurements performed in October until December 2003 of up to 400 pptv as well.

The monthly mean mixing ratios (bins of 5 times 15°) reveal a global background of about 40 pptv or 50 pptv while maximum values reach up to 200 pptv in October 2007 in 12 km above the southern Altantic Ocean, and some other regions as well (see Fig. 13). Monthly means of MIPAS HR C_2H_2 retrievals for August 2003 in 200 hPa retrieved by Parker et al. (2011) show peak (approx. 200 pptv) and background (approx. 50 pptv) mixing ratios very close to our MIPAS RR monthly mean mixing ratios.

Singh et al. (1996) measured median mixing ratios in polluted air masses by in situ measurements above the southern Atlantic Ocean of 160 pptv and 50 pptv as background at 11.5 km in September and October 1992. González Abad et al. (2011) reported long-term and global averaged mixing ratios profiles of C_2H_2 measured by ACE. In 12 km mixing ratios of 52 pptv have been obtained, in 8 km 70 pptv respectively. Again, MIPAS is in reasonable agreement with these independent measurements. The contrast in-plume and outside of plume measurements often is 150 pptv which exceeds the single measurement precision by a factor of seven, suggesting that MIPAS can measure the C_2H_2 variability (Table 5).

4.3 HCN

HCN is well mixed in the troposphere and has slowly decreasing mixing ratios due to loss by reaction with OH and O(1D) in the stratosphere (Cicerone and Zellner, 1983). Spaceborne measurements (Rinsland et al., 1998) led to the conclusion that HCN mainly is produced by biomass burning and may be utilised as a tracer for such events (Singh et al., 2001; Li et al., 2003; Glatthor et al., 2007).

HCN at the sample orbit (Fig. 14) exhibits mixing ratios of about 200 pptv at lowermost altitudes close to the tropopause throughout all latitudes. Polluted air masses show mixing ratios up to 1 ppbv. Glatthor et al. (2009) obtained mixing ratios of about 300 pptv by HR single measurements at all latitudes and longitudes at 12 km altitude. HR peak values reach 500 pptv. Atmospheric Trace Molecule Spectroscopy (ATMOS) measurements (Rinsland et al., 1998)

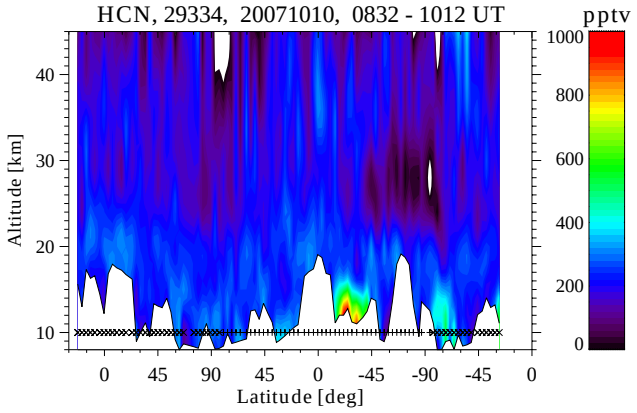

Fig. 14. As Fig. 9 but for HCN.

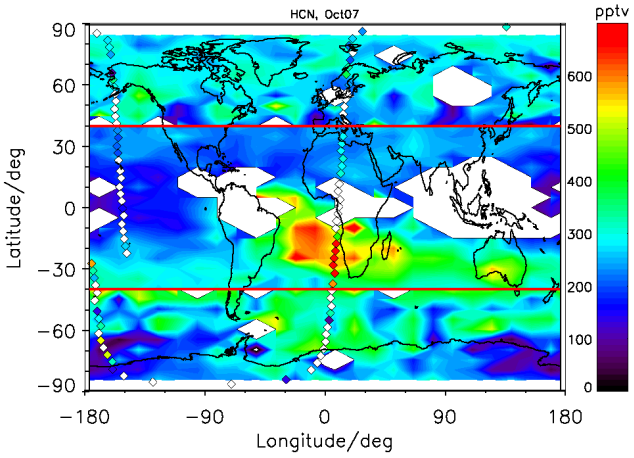

Fig. 15. As Fig. 10 but for HCN.

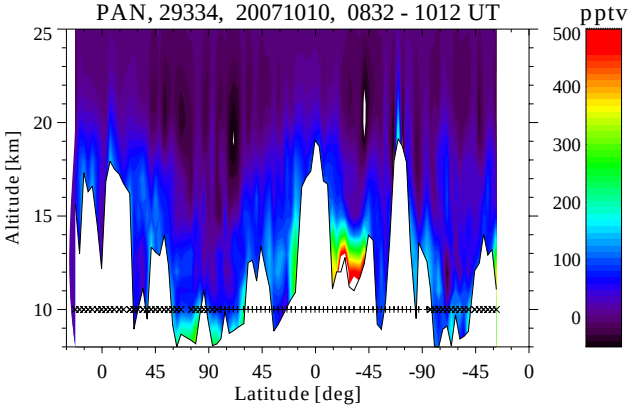

Fig. 16. As Fig. 9 but for PAN.

revea mixing ratios close to 1 ppbv at one measurement and above 400 pptv for a few others at comparable altitudes while background values are between 200 and 300 pptv. ACE measured HCN mixing ratios ranging from 190 pptv to some exceptional peak values of up to 600 pptv in July 2004 below the tropopause in northern midlatitudes (Rinsland et al., 2007). MIPAS measurements fall within this range.

The differences of mixing ratios between locations inside and outside of biomass burning plumes are often in the order of 400 pptv (Table 5). This significantly exceeds the MIPAS single profile measurement precision.

While the HR measurements performed by Glatthor et al. (2009) for October 2003 reach monthly means of 500 pptv, the RR mixing ratios exceed 600 pptv above the southern Atlantic Ocean in October 2007 at 12 km (Fig. 15) at the same altitude. Regional enhancements of HCN polewards of 40° at 8 km are found in both hemispheres. They are presumed to be advected from biomass burning events at lower latitudes or boreal fires.

The MIPAS RR five-year data set of zonal means (not shown) is characterised by a large interannual variability with maximum values from 380 pptv (2006) to 550 pptv (2007) at northern midlatitudes and 8 km and from 340 pptv (2006) to 580 pptv (2007) at southern midlatitudes. Thus, the differences between MIPAS HR and RR analyses and the difference between ATMOS and MIPAS do not hint at any bias but are within the range of natural variability.

4.4 PAN

Peroxyacetyl nitrate (PAN) is produced from tropospheric precursors. The precursors are hydrocarbons which have been transformed at different steps to the peroxyacetyl radical $CH_3C(O)OO$. A reversible reaction of the peroxyacetyl radical with nitrate (NO_2) leads to PAN. The lifetime of PAN is strongly temperature dependent (Singh, 1987) with up to 5 months at 250 K and about an hour at 298 K. Thus the lifetime at the tropopause level exceeds the lifetime in lower troposphere and upper stratosphere.

Peak mixing ratios of PAN measured by MIPAS at reduced spectral resolution reach more than 500 pptv. At several other locations mixing ratios up to 250 pptv are obtained (Fig. 16). At polluted areas, e.g. over the southern Atlantic Ocean at 12 km, PAN monthly mean mixing ratios exceed 400 pptv. The RR monthly mean mixing ratios show background values of about 100 pptv except of northern midlatitudes and polar regions (Fig. 17). There, more than 200 pptv are reached at most locations. Larger PAN mixing ratios in the Northern than the Southern hemisphere reflect the larger abundances of its anthropogenic precursers in the Northern hemisphere (see e.g. Fig. 10).

Upper tropospheric ten-day mean PAN mixing ratios in October 2003, which falls in the MIPAS HR period, reach 500 pptv (Glatthor et al., 2007); their tropospheric background mixing ratios were below 100 pptv at southern latitudes and about 150 at northern latitudes. Further MIPAS HR retrievals were performed by Moore and Remedios (2010). These authors found similar backgrounds at global monthly means in January 2003. Their peak values are close to 500 pptv at 300 hPa and about 225 pptv at 201 hPa. These HR

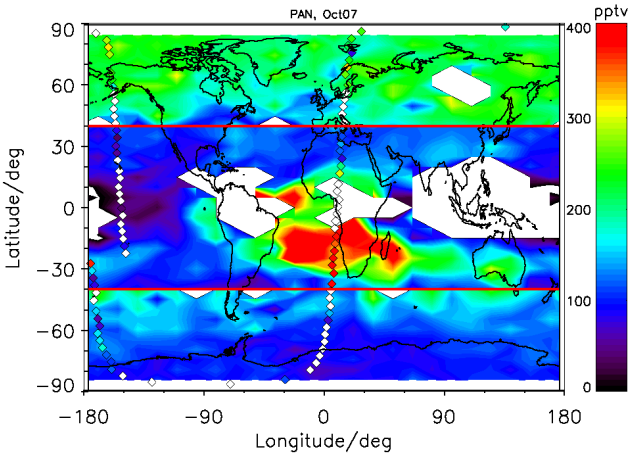

Fig. 17. As Fig. 10 but for PAN.

results are in good agreement to our PAN results retrieved from MIPAS RR spectra. Also for PAN, the interannual variability is larger than the differences between the data sets compared.

Furthermore, Singh et al. (1996) measured in situ at 12 km of altitude median mixing ratios of about 100 pptv as background and above 300 pptv at polluted air masses in September and October 1992.

The amplitude of the annual cycle of monthly zonal means in northern midlatitudes (not shown) is in the order of 250 pptv in 8 km altitude and of 150 pptv in 12 km. The local small scale variability of monthly means between inside and outside of a biomass burning plume is often about 350 pptv (Table 5). Thus the temporal and the local variability exceeds the single measurement precision at least by a factor of five.

5 Conclusions and outlook

MIPAS onboard Envisat is able to measure pollutants in the upper troposphere also at reduced spectral resolution which is applied since beginning of 2005. HCN, PAN, and C_2H_2 can be measured with a slightly better altitude resolution compared to the high spectral resolution mode at most levels. Only the C_2H_6 measurements have a reduced altitude resolution. The improvements refer particularly to the upper troposphere.

In case of significantly enhanced mixing ratios, like in biomass burning plumes, the total relative random errors of all species under assessment are 15 % or below. This means that plumes can be clearly distinguished from clean background air. The similar spatial extent of the plumes as inferred from the four species under investigation adds up to a self-consistent picture and provides confidence in the results. Comparison of the distributions reveals that even minor structures are often highly correlated between the gases (e.g. peaks over Madagascar, double peak over Southern Africa, local enhancement over Southern Australia). However, there are also pronounced differences which deserve to be investigated in future studies: while, e.g. C_2H_6 and C_2H_2 are notably increased over the Tibetan Plateau, HCN and PAN show much less pronounced enhancements there.

The retrieved mixing ratios at reduced spectral resolution are in good agreement with the mixing ratios obtained by high resolution measurements or measured by other instruments. No indication for inconsistency between the different measurements has been detected. Comparison with results found in literature suggests that the chemical characteristics of biomass burning plumes with respect to C_2H_6, C_2H_2, HCN, and PAN have been quite similar in the time periods analyzed. In this study, all four gases were analyzed for the period from January 2005 to January 2010, and these gases are now included in the routine processing at IMK.

Acknowledgements. The work was funded by DFG under contract number GL 643/1-1, project POMODORO. ESA has provided MIPAS level-1 data. The retrievals of IMK/IAA were partly performed on the HP XC4000 of the Scientific Supercomputing Center (SSC) Karlsruhe under project grant MIPAS. IMK data analysis was supported by DLR under contract number 50EE0901.

Edited by: M. Riese

References

Aikin, A. C., Herman, J. R., Maier, E. J., and McQuillan, C. J.: Atmospheric Chemistry of Ethane and Ethylene, J. Geophys. Res., 87, 3105–3118, 1982.

Allen, G., Remedios, J. J., Newnham, D. A., Smith, K. M., and Monks, P. S.: Improved mid-infrared cross-sections for peroxyacetyl nitrate (PAN) vapour, Atmos. Chem. Phys., 5, 47–56, doi:10.5194/acp-5-47-2005, 2005.

Chatfield, R. B., Vastano, J. A., Li, L., Sachse, G. W., and Connors, V. S.: The Great African plume from biomass burning, in: Generalizations from a three-dimensional study of TRACE A carbon monoxide, J. Geophys. Res., 103, 28059–28077, 1998.

Cicerone, R. J. and Zellner, R.: The Atmospheric Chemistry of Hydrogen Cyanide (HCN), J. Geophys. Res., 88, 10689–10696, 1983.

Coheur, P.-F., Herbin, H., Clerbaux, C., Hurtmans, D., Wespes, C., Carleer, M., Turquety, S., Rinsland, C. P., Remedios, J., Hauglustaine, D., Boone, C. D., and Bernath, P. F.: ACE-FTS observation of a young biomass burning plume: first reported measurements of C_2H_4, C_3H_6O, H_2CO and PAN by infrared occultation from space, Atmos. Chem. Phys., 7, 5437–5446, doi:10.5194/acp-7-5437-2007, 2007.

Coheur, P.-F., Clarisse, L., Turquety, S., Hurtmans, D., and Clerbaux, C.: IASI measurements of reactive trace species in biomass burning plumes, Atmos. Chem. Phys., 9, 5655–5667, doi:10.5194/acp-9-5655-2009, 2009.

Echle, G., von Clarmann, T., Dudhia, A., Flaud, J.-M., Funke, B., Glatthor, N., Kerridge, B., López-Puertas, M., Martín-Torres, F. J., and Stiller, G. P.: Optimized spectral microwindows for data analysis of the Michelson Interferometer for Passive

Atmospheric Sounding on the Environmental Satellite, Appl. Optics, 39, 5531–5540, 2000.

Fischer, H., Birk, M., Blom, C., Carli, B., Carlotti, M., von Clarmann, T., Delbouille, L., Dudhia, A., Ehhalt, D., Endemann, M., Flaud, J. M., Gessner, R., Kleinert, A., Koopman, R., Langen, J., López-Puertas, M., Mosner, P., Nett, H., Oelhaf, H., Perron, G., Remedios, J., Ridolfi, M., Stiller, G., and Zander, R.: MIPAS: an instrument for atmospheric and climate research, Atmos. Chem. Phys., 8, 2151–2188, doi:10.5194/acp-8-2151-2008, 2008.

Glatthor, N., von Clarmann, T., Fischer, H., Funke, B., Grabowski, U., Höpfner, M., Kellmann, S., Kiefer, M., Linden, A., Milz, M., Steck, T., and Stiller, G. P.: Global peroxyacetyl nitrate (PAN) retrieval in the upper troposphere from limb emission spectra of the Michelson Interferometer for Passive Atmospheric Sounding (MIPAS), Atmos. Chem. Phys., 7, 2775–2787, doi:10.5194/acp-7-2775-2007, 2007.

Glatthor, N., von Clarmann, T., Stiller, G. P., Funke, B., Koukouli, M. E., Fischer, H., Grabowski, U., Höpfner, M., Kellmann, S., and Linden, A.: Large-scale upper tropospheric pollution observed by MIPAS HCN and C_2H_6 global distributions, Atmos. Chem. Phys., 9, 9619–9634, doi:10.5194/acp-9-9619-2009, 2009.

González Abad, G., Allen, N. D. C., Bernath, P. F., Boone, C. D., McLeod, S. D., Manney, G. L., Toon, G. C., Carouge, C., Wang, Y., Wu, S., Barkley, M. P., Palmer, P. I., Xiao, Y., and Fu, T. M.: Ethane, ethyne and carbon monoxide concentrations in the upper troposphere and lower stratosphere from ACE and GEOS-Chem: a comparison study, Atmos. Chem. Phys., 11, 9927–9941, doi:10.5194/acp-11-9927-2011, 2011.

Kiefer, M., Arnone, E., Dudhia, A., Carlotti, M., Castelli, E., von Clarmann, T., Dinelli, B. M., Kleinert, A., Linden, A., Milz, M., Papandrea, E., and Stiller, G.: Impact of temperature field inhomogeneities on the retrieval of atmospheric species from MIPAS IR limb emission spectra, Atmos. Meas. Tech., 3, 1487–1507, doi:10.5194/amt-3-1487-2010, 2010.

Li, Q., Jacob, D. J., Yantosca, R. M., Heald, C. L., Singh, H. B., Koike, M., Zhao, Y., Sachse, G. W., and Streets, D. G.: A global three-dimensional model analysis of the atmospheric budgets of HCN and CH_3CN: Constraints from aircraft and ground measurements, J. Geophys. Res., 108, 8827, doi:10.1029/2002JD003075, 2003.

Li, Q., Palmer, P. I., Pumphrey, H. C., Bernath, P., and Mahieu, E.: What drives the observed variability of HCN in the troposphere and lower stratosphere?, Atmos. Chem. Phys., 9, 8531–8543, doi:10.5194/acp-9-8531-2009, 2009.

Liang, Q., Jaegle, L., Hudman, R. C., Turquety, S., Jacob, D. J., Avery, M. A., Browell, E. V., Sachse, G. W., Blake, D. R., Brune, W., Ren, X., Cohen, R. C., Dibb, J. E., Fried, A., Fuelberg, H., Porter, M., Heikes, B. G., Huey, G., Singh, H. B., and Wennberg, P. O.: Summertime influence of Asian pollution in the free troposphere over North America, J. Geophys. Res., 112, D12S11, doi:10.1029/2006JD007919, 2007.

Moore, D. P. and Remedios, J. J.: Seasonality of Peroxyacetyl nitrate (PAN) in the upper troposphere and lower stratosphere using the MIPAS-E instrument, Atmos. Chem. Phys., 10, 6117–6128, doi:10.5194/acp-10-6117-2010, 2010.

Norton, R. H. and Beer, R.: New apodizing functions for Fourier spectrometry, J. Opt. Soc. Am., 66, 259–264, 1976.

Parker, R. J., Remedios, J. J., Moore, D. P., and Kanawade, V. P.: Acetylene C_2H_2 retrievals from MIPAS data and regions of enhanced upper tropospheric concentrations in August 2003, Atmos. Chem. Phys., 11, 10243–10257, doi:10.5194/acp-11-10243-2011, 2011.

Pumphrey, H. C., Jimenez, C. J., and Waters, J. W.: Measurement of HCN in the middle atmosphere by EOS MLS, Geophys. Res. Lett., 33, L08804, doi:10.1029/2005GL025656, 2006.

Randel, W. J., Park, M., Emmons, L., Kinnison, D., Bernath, P., Walker, K. A., Boone, C., and Pumphrey, H.: Asian Monsoon Transport of Pollution to the Stratosphere, Science, 328, 611–613, doi:10.1126/science.1182274, 2010.

Rinsland, C. P., Zander, R., Farmer, C. B., Norton, R. H., and Russell III, J. M.: Concentration of ethane (C_2H_6) in the lower stratosphere and upper troposphere and acetylene (C_2H_2) in the upper troposphere deduced from atmospheric trace molecule spectroscopy/Spacelab 3 spectra, J. Geophys. Res., 92, 11951–11964, 1987.

Rinsland, C. P., Gunson, M. R., Wang, P.-H., Arduini, R. F., Baum, B. A., Minnis, P., Goldman, A., Abrams, M. C., Zander, R., Mahieu, E., Salawitch, R. J., Michelsen, H. A., Irion, F. W., and Newchurch, M. J.: ATMOS/ATLAS 3 Infrared Measurements of Trace Gases in the November 1994 Tropical and Subtropical Upper Troposphere, J. Quant. Spectrosc. Ra., 60, 891–901, 1998.

Rinsland, C. P., Duffour, G., Boone, C. D., Bernath, P. F., and Chiou, L.: Atmospheric Chemistry Experiment (ACE) measurements of elevated Southern Hemisphere upper tropospheric CO, C_2H_6, HCN, and C_2H_2 mixing ratios from biomass burning emissions and long-range transport, Geophys. Res. Lett., 32, L20803, doi:10.1029/2005GL024214, 2005.

Rinsland, C. P., Dufour, G., Boone, C. D., Bernath, P. F., Chiou, L., Coheur, P.-F., Turquety, S., and Clerbaux, C.: Satellite boreal measurements over Alaska and Canada during June–July 2004: Simultaneous measurements of upper tropospheric CO, C_2H_6, HCN, CH_3Cl, CH_4, CH_3OH, HCOOH, OCS, and SF_6 mixing ratios, Global Biogeochem. Cy., 21, GB3008, doi:1029/2006GB002795, 2007.

Rothman, L. S., Jacquemart, D., Barbe, A., Chris Benner, D., Birk, M., Brown, L. R., Carleer, M. R., Chackerian Jr., C., Chance, K., Coudert, L. H., Dana, V., Devi, V. M., Flaud, J.-M., Gamache, R. R., Goldman, A., Hartmann, J.-M., Jucks, K. W., Maki, A. G., Mandin, J.-Y., Massie, S. T., Orphal, J., Perrin, A., Rinsland, C. P., Smith, M. A. H., Tennyson, J., Tolchenov, R. N., Toth, R. A., Vander Auwera, J., Varanasi, P., and Wagner, G.: The HITRAN 2004 molecular spectroscopic database, J. Quant. Spectrosc. Ra., 96, 139–204, doi:10.1016/j.jqsrt.2004.10.008, 2005.

Rudolph, J.: The tropospheric distribution and budget of ethane, J. Geophys. Res., 100, 11369–11381, 1995.

Shim, C., Li, Q., Luo, M., Kulawik, S., Worden, H., Worden, J., Eldering, A., Diskin, G., Sachse, G., Weinheimer, A., Knapp, D., Montzca, D., and Campos, T.: Characterizing mega-city pollution with TES O_3 and CO measurements, Atmos. Chem. Phys. Discuss., 7, 15189–15212, doi:10.5194/acpd-7-15189-2007, 2007.

Singh, H.: Reactive nitrogen in the troposphere, Environ. Sci. Technol., 21, 320–327, 1987.

Singh, H. B., Herlth, D., Kolyer, R., Chatfield, R., Viezee, W., Salas, L. J., Chen, Y., Bradshaw, J. D., Sandholm, S. T., Talbot, R., Gregory, G. L., Anderson, B., Sachse, G. W., Browell, E., Bachmeier, A. S., Blake, D. R., Heikes, B., Jacob, D., and Fuelberg, H. E.: Impact of biomass burning emissions on the composition of the South Atlantic troposphere: Reactive nitrogen and ozone, J. Geophys. Res., 101, 24203–24219, 1996.

Singh, H., Chen, Y., Staudt, A., Jacob, D., Blake, D., Heikes, B., and Snow, J.: Evidence from the Pacific troposphere for large global sources of oxygenated organic compounds, Nature, 410, 1078, doi:10.1038/35074067, 2001.

Spang, R., Remedios, J. J., and Barkley, M. P.: Colour indices for the detection and differentiation of cloud types in infra-red limb emission spectra, Adv. Space. Res., 33, 1041–1047, 2004.

Steck, T., and von Clarmann, T.: Constrained Profile Retrieval Applied to the Observation Mode of the Michelson Interferometer for Passive Atmospheric Sounding, Appl. Optics, 40, 3559–3571, 2001.

Stiller, G. P., von Clarmann, T., Funke, B., Glatthor, N., Hase, F., Höpfner, M., and Linden, A.: Sensitivity of trace gas abundances retrievals from infrared limb emission spectra to simplifying approximations in radiative transfer modelling, J. Quant. Spectrosc. Ra., 72, 249–280, 2002.

Talbot, R. W., Dibb, J. E., Klemm, K. I., Bradshaw, J. D., Sandholm, S. T., Blake, D. R., Sachse, G. W., Collins, J., Heikes, B. G., Gregory, G. L., Anderson, B. E., Singh, H. B., Thornton, D. C., and Merrill, J. T.: Chemical characteristics of continental outflow from Asia to the troposphere over theWestern Pacific Ocean during September–October 1991: results from PEM-West A, J. Geophys. Res., 101, 1713–1725, 1996.

Tikhonov, A.: On the solution of incorrectly stated problems and method of regularization, Dokl. Akad. Nauk. SSSR, 151, 501–504, 1963.

von Clarmann, T., and Echle, G.: Selection of Optimized Microwindows for Atmospheric Spectroscopy, Appl. Optics, 37, 7661–7669, 1998.

von Clarmann, T., Glatthor, N., Grabowski, U., Höpfner, M., Kellmann, S., Kiefer, M., Linden, A., Mengistu Tsidu, G., Milz, M., Steck, T., Stiller, G. P., Wang, D. Y., Fischer, H., Funke, B., Gil-López, S., and López-Puertas, M.: Retrieval of temperature and tangent altitude pointing from limb emission spectra recorded from space by the Michelson Interferometer for Passive Atmospheric Sounding (MIPAS), J. Geophys. Res., 108, 4736, doi:10.1029/2003JD003602, 2003.

von Clarmann, T., Glatthor, N., Koukouli, M. E., Stiller, G. P., Funke, B., Grabowski, U., Höpfner, M., Kellmann, S., Linden, A., Milz, M., Steck, T., and Fischer, H.: MIPAS measurements of upper tropospheric C_2H_6 and O_3 during the southern hemispheric biomass burning season in 2003, Atmos. Chem. Phys., 7, 5861–5872, doi:10.5194/acp-7-5861-2007, 2007.

von Clarmann, T., De Clercq, C., Ridolfi, M., Höpfner, M., and Lambert, J.-C.: The horizontal resolution of MIPAS, Atmos. Meas. Tech., 2, 47–54, doi:10.5194/amt-2-47-2009, 2009a.

von Clarmann, T., Höpfner, M., Kellmann, S., Linden, A., Chauhan, S., Funke, B., Grabowski, U., Glatthor, N., Kiefer, M., Schieferdecker, T., Stiller, G. P., and Versick, S.: Retrieval of temperature, H_2O, O_3, HNO_3, CH_4, N_2O, $ClONO_2$ and ClO from MIPAS reduced resolution nominal mode limb emission measurements, Atmos. Meas. Tech., 2, 159–175, doi:10.5194/amt-2-159-2009, 2009b.

Wolfe, G. M., Thornton, J. A., McNeill, V. F., Jaffe, D. A., Reidmiller, D., Chand, D., Smith, J., Swartzendruber, P., Flocke, F., and Zheng, W.: Influence of trans-Pacific pollution transport on acyl peroxy nitrate abundances and speciation at Mount Bachelor Observatory during INTEX-B, Atmos. Chem. Phys., 7, 5309–5325, doi:10.5194/acp-7-5309-2007, 2007.

Xiao, Y., Jacob, D. J., and Turquety, S.: Atmospheric acetylene and its relationship with CO as an indicator of air mass age, J. Geophys. Res., 112, D12305, doi:10.1029/2006JD008268, 2007.

Xiao, Y., Logan, J. A., Jacob, D. J., Hudman, R. C., Yantosca, R., and Blake, D. R.: Global budget of ethane and regional constraints on US sources, J. Geophys. Res., 113, D21306, doi:10.1029/2007JD009415, 2008.